



Article

Effect of MgCl₂ and GdCl₃ on ORAI1 Expression and Store-Operated Ca²⁺ Entry in Megakaryocytes

Kuo Zhou ¹, Xuexue Zhu ¹, Ke Ma ¹ , Jibin Liu ², Bernd Nürnberg ¹ , Meinrad Gawaz ³ and Florian Lang ^{4,*}

¹ Department of Pharmacology, Experimental Therapy & Toxicology, Eberhard Karls University, 72074 Tübingen, Germany; azh.zhoukuo@gmail.com (K.Z.); xuexue.zhu1992@gmail.com (X.Z.); mke_card@163.com (K.M.); bernd.nuernberg@uni-tuebingen.de (B.N.)

² Institute of Preventive Veterinary Medicine, Key Laboratory of Animal Disease and Human Health of Sichuan Province, Sichuan Agricultural University, Chengdu 611130, China; eaeas12@163.com

³ Department of Cardiology and Angiology, University Hospital Tübingen, Eberhard Karls University Tübingen, 72076 Tübingen, Germany; meinrad.gawaz@med.uni-tuebingen.de

⁴ Department of Vegetative and Clinical Physiology, Eberhard Karls University, 72074 Tübingen, Germany

* Correspondence: florian.lang@uni-tuebingen.de; Tel.: +49-707-129-72194

Abstract: In chronic kidney disease, hyperphosphatemia upregulates the Ca²⁺ channel ORAI and its activating Ca²⁺ sensor STIM in megakaryocytes and platelets. ORAI1 and STIM1 accomplish store-operated Ca²⁺ entry (SOCE) and play a key role in platelet activation. Signaling linking phosphate to upregulation of ORAI1 and STIM1 includes transcription factor NFAT5 and serum and glucocorticoid-inducible kinase SGK1. In vascular smooth muscle cells, the effect of hyperphosphatemia on ORAI1/STIM1 expression and SOCE is suppressed by Mg²⁺ and the calcium-sensing receptor (CaSR) agonist Gd³⁺. The present study explored whether sustained exposure to Mg²⁺ or Gd³⁺ interferes with the phosphate-induced upregulation of NFAT5, SGK1, ORAI1,2,3, STIM1,2 and SOCE in megakaryocytes. To this end, human megakaryocytic Meg-01 cells were treated with 2 mM β-glycerophosphate for 24 h in the absence and presence of either 1.5 mM MgCl₂ or 50 μM GdCl₃. Transcript levels were estimated utilizing q-RT-PCR, protein abundance by Western blotting, cytosolic Ca²⁺ concentration ([Ca²⁺]_i) by Fura-2 fluorescence and SOCE from the increase in [Ca²⁺]_i following re-addition of extracellular Ca²⁺ after store depletion with thapsigargin (1 μM). As a result, Mg²⁺ and Gd³⁺ upregulated CaSR and blunted or virtually abolished the phosphate-induced upregulation of NFAT5, SGK1, ORAI1,2,3, STIM1,2 and SOCE in megakaryocytes. In conclusion, Mg²⁺ and the CaSR agonist Gd³⁺ interfere with phosphate-induced dysregulation of [Ca²⁺]_i in megakaryocytes.



Citation: Zhou, K.; Zhu, X.; Ma, K.; Liu, J.; Nürnberg, B.; Gawaz, M.; Lang, F. Effect of MgCl₂ and GdCl₃ on ORAI1 Expression and Store-Operated Ca²⁺ Entry in Megakaryocytes. *Int. J. Mol. Sci.* **2021**, *22*, 3292. <https://doi.org/10.3390/ijms22073292>

Academic Editor: Valeria Gasperi

Received: 15 February 2021

Accepted: 18 March 2021

Published: 24 March 2021

Publisher's Note: MDPI stays neutral with regard to jurisdictional claims in published maps and institutional affiliations.



Copyright: © 2021 by the authors. Licensee MDPI, Basel, Switzerland. This article is an open access article distributed under the terms and conditions of the Creative Commons Attribution (CC BY) license (<https://creativecommons.org/licenses/by/4.0/>).

Keywords: SOCE; ORAI1,2,3; STIM1,2; SGK1; NFAT5; Mg²⁺; Gd³⁺; calcium-sensing receptor; megakaryocytes

1. Introduction

The impairment of renal phosphate excretion in chronic kidney disease (CKD) increases the plasma phosphate concentration with subsequent osteogenic reprogramming of vascular smooth muscle cells (VSMCs) [1–4] and vascular calcification [5–8]. Underlying signaling includes nuclear factor of activated T cells 5 (NFAT5) [9–12], serum and glucocorticoid-inducible kinase 1 (SGK1) [13,14] and Ca²⁺ channel ORAI with its activator stromal interaction molecule (STIM) [15–17]. Opening of ORAI by STIM upon intracellular Ca²⁺ depletion results in store-operated Ca²⁺ entry (SOCE) [15], which contributes to the orchestration of vascular calcification [16–18] as well as mineralization of bone [19] and enamel [20,21].

NFAT5, SGK1 and ORAI1/STIM1 similarly participate in activation of blood platelets [22–27] and thus contribute to the development of thrombosis and thrombo-occlusive events [23,26,27]. Platelets are generated by megakaryocytes, and protein abundance in platelets depends on megakaryocytic transcript and protein expression [28,29]. Megakaryocytes express ORAI1,

ORAI2 and ORAI3 [30], thus accomplishing SOCE [31–34]. ORAI expression and SOCE are upregulated by the phosphate donor β -glycerophosphate [30]. The stimulation of vascular calcification by phosphate has been shown to be reversed by Mg^{2+} and the calcium-sensing receptor (CaSR) agonist Gd^{3+} [17,35].

Expression of the calcium-sensing receptor has previously been shown in both megakaryocytes and platelets [36]. CaSR activation has been shown to counteract activation of blood platelets in hyperhomocysteinemia [37]. However, to the best of our knowledge, a functional role of CaSR in megakaryocytes and a role of CaSR in the regulation of ORAI1/STIM1 abundance and activity of megakaryocytes and platelets have never been reported before. The present paper thus explored whether Mg^{2+} or Gd^{3+} modifies NFAT5, SGK1, ORAI1,2,3 and STIM1,2 expression as well as SOCE in megakaryocytes without or with prior exposure to phosphate donor β -glycerophosphate.

2. Results

In the first set of experiments, RT-PCR was employed to quantify transcript levels encoding the calcium-sensing receptor (*CaSR*), the transcription factor *NFAT5*, the NFAT5-regulated *SGK1*, the SGK1-sensitive Ca^{2+} release-activated ion channels *ORAI1*, *ORAI2* and *ORAI3* and the ORAI-activating Ca^{2+} sensor isoforms *STIM1* and *STIM2*. According to RT-PCR (Figure S1), *ORAI1* was, by far, the predominant ORAI isoform and *STIM1* the prevailing *STIM* isoform. As shown in Figure 1, $MgCl_2$ treatment significantly upregulated *CaSR* expression with or without prior exposure to β -glycerophosphate. In agreement with earlier observations [30], a 24-h pretreatment of human megakaryocytes with the phosphate donor β -glycerophosphate upregulated the transcript levels of *NFAT5*, *SGK1*, *ORAI1*, *ORAI2*, *ORAI3*, *STIM1* and *STIM2*. All those effects were significantly blunted or virtually abrogated by additional exposure to 1.5 mM $MgCl_2$. In the absence of β -glycerophosphate, $MgCl_2$ did not significantly modify the transcript levels of *NFAT5*, *SGK1*, *ORAI1*, *ORAI2*, *ORAI3*, *STIM1* and *STIM2* (Figure 1).

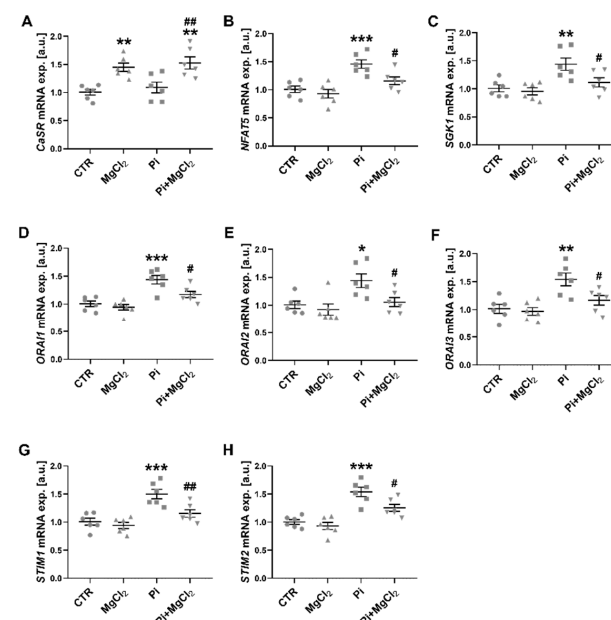


Figure 1. Upregulation of *CaSR* transcription by $MgCl_2$ and reversal of β -glycerophosphate-induced *NFAT5*, *SGK1*, *ORAI1*, *ORAI2*, *ORAI3*, *STIM1* and *STIM2* transcription in megakaryocytes by $MgCl_2$. (A–H) Arithmetic means (\pm SEM, $n = 6$) of *CaSR* (A), *NFAT5* (B), *SGK1* (C), *ORAI1* (D), *ORAI2* (E), *ORAI3* (F), *STIM1* (G) and *STIM2* (H) transcript levels in megakaryocytes without (CTR) and with prior 24-h exposure to 1.5 mM $MgCl_2$ alone ($MgCl_2$), 2 mM β -glycerophosphate alone (Pi) or 2 mM β -glycerophosphate and 1.5 mM $MgCl_2$ (Pi+ $MgCl_2$). * ($p < 0.05$), ** ($p < 0.01$), *** ($p < 0.001$) indicate statistically significant differences compared to CTR; # ($p < 0.05$), ## ($p < 0.01$) indicate statistically significant differences compared to Pi alone (ANOVA). CaSR, calcium-sensing receptor; CTR, control.

Western blots were performed to test whether the observed alterations in ORAI1 and STIM1 transcript levels are paralleled by the respective changes in ORAI1 and STIM1 protein abundance. As illustrated in Figure 2, β -glycerophosphate upregulated the ORAI1 and STIM1 protein abundance, an effect significantly blunted by additional exposure to 1.5 mM MgCl_2 . Again, in the absence of β -glycerophosphate, MgCl_2 did not significantly modify the ORAI1 and STIM1 protein abundance (Figure 2).

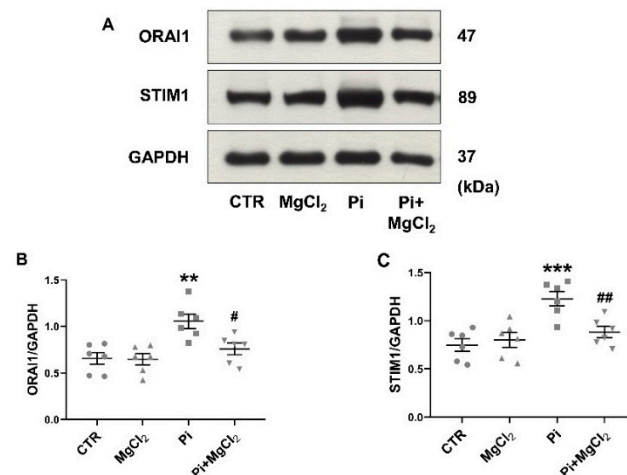


Figure 2. Reversal of β -glycerophosphate-induced ORAI1 and STIM1 protein expression in megakaryocytes by MgCl_2 . (A) Original Western blots of ORAI1, STIM1 and GAPDH protein abundance in megakaryocytes without (CTR) and with prior 24-h exposure to 1.5 mM MgCl_2 alone (MgCl_2), 2 mM β -glycerophosphate alone (Pi) or 2 mM β -glycerophosphate and 1.5 mM MgCl_2 (Pi+ MgCl_2). (B,C) Arithmetic means \pm SEM ($n = 6$) of ORAI1 (B) and STIM1 (C) protein abundance in megakaryocytes without (CTR) and with prior 24-h exposure to 1.5 mM MgCl_2 alone (MgCl_2), 2 mM β -glycerophosphate alone (Pi) or 2 mM β -glycerophosphate and 1.5 mM MgCl_2 (Pi+ MgCl_2). ** ($p < 0.01$), *** ($p < 0.001$) indicate statistically significant differences compared to CTR; # ($p < 0.05$), ## ($p < 0.01$) indicate statistically significant differences compared to Pi alone (ANOVA). CTR, control.

Cytosolic Ca^{2+} activity ($[\text{Ca}^{2+}]_i$) was estimated utilizing Fura-2 fluorescence to test whether the enhanced expression of ORAI and STIM is followed by the respective alterations in store-operated Ca^{2+} entry (SOCE). The 340 nm/380 nm ratio reflecting $[\text{Ca}^{2+}]_i$ was, prior to store depletion, similar in β -glycerophosphate-treated (1.298 ± 0.086 , $n = 6$) and untreated (1.202 ± 0.094 , $n = 6$) megakaryocytes. For determination of SOCE, cells were exposed to thapsigargin (1 μM), a sarco/endoplasmic reticulum Ca^{2+} /ATPase (SERCA) inhibitor, and Ca^{2+} -free solutions to deplete intracellular Ca^{2+} stores. In the following, extracellular Ca^{2+} was re-added in the continued presence of thapsigargin to quantify SOCE from the increase in $[\text{Ca}^{2+}]_i$. As illustrated in Figure 3, β -glycerophosphate pretreatment significantly increased both the peak and the slope of SOCE, an effect significantly blunted by additional exposure to 1.5 mM MgCl_2 . Again, in the absence of β -glycerophosphate, MgCl_2 did not significantly modify SOCE. Neither β -glycerophosphate nor MgCl_2 significantly modified Ca^{2+} release.

Additional experiments were performed to test whether the effects of MgCl_2 were mimicked by calcium-sensing receptor agonist Gd^{3+} . As illustrated in Figure 4, *CaSR* transcription was significantly upregulated by the exposure to 50 μM GdCl_3 both in the absence and presence of β -glycerophosphate. The upregulation of *NFAT5*, *SGK1*, *ORAI1*, *ORAI2*, *ORAI3*, *STIM1* and *STIM2* transcript levels by 2 mM β -glycerophosphate was significantly blunted by additional exposure to 50 μM GdCl_3 . In the absence of β -glycerophosphate, 50 μM GdCl_3 did not significantly modify the transcript levels of *NFAT5*, *SGK1*, *ORAI1*, *ORAI2*, *ORAI3*, *STIM1* and *STIM2* (Figure 4).

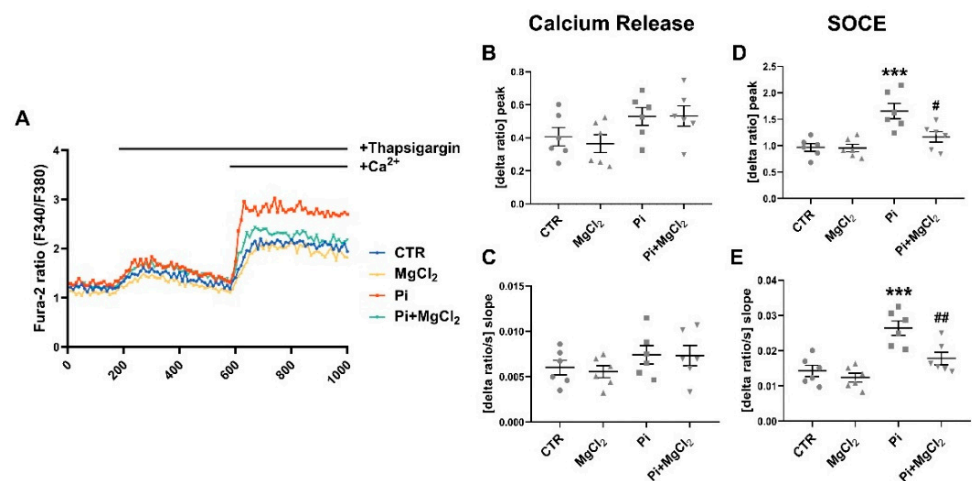


Figure 3. Reversal of β -glycerophosphate-induced increase in store-operated Ca^{2+} entry (SOCE) in megakaryocytes by MgCl_2 . (A) Representative tracings of Fura-2 fluorescence ratio in fluorescence spectrometry before and following extracellular Ca^{2+} removal and addition of thapsigargin ($1 \mu\text{M}$) as well as re-addition of extracellular Ca^{2+} in megakaryocytes without (CTR) or with prior 24-h exposure to 1.5 mM MgCl_2 alone (MgCl_2), 2 mM β -glycerophosphate alone (Pi) or 2 mM β -glycerophosphate and 1.5 mM MgCl_2 (Pi+ MgCl_2). (B,C) Arithmetic means ($\pm\text{SEM}$, $n = 6$) of peak (B) and slope (C) increase in Fura-2 fluorescence ratio following addition of thapsigargin ($1 \mu\text{M}$) in megakaryocytes without (CTR) or with prior 24-h exposure to 1.5 mM MgCl_2 alone (MgCl_2), 2 mM β -glycerophosphate alone (Pi) or 2 mM β -glycerophosphate and 1.5 mM MgCl_2 (Pi+ MgCl_2). (D,E) Arithmetic means ($\pm\text{SEM}$, $n = 6$) of peak (D) and slope (E) increase in Fura-2 fluorescence ratio following re-addition of extracellular Ca^{2+} in megakaryocytes without (CTR) or with prior 24-h exposure to 1.5 mM MgCl_2 alone (MgCl_2), 2 mM β -glycerophosphate alone (Pi) or 2 mM β -glycerophosphate and 1.5 mM MgCl_2 (Pi+ MgCl_2). *** ($p < 0.001$) indicates statistically significant difference compared to CTR; # ($p < 0.05$), ## ($p < 0.01$) indicate statistically significant differences compared to Pi alone (ANOVA). CTR, control.

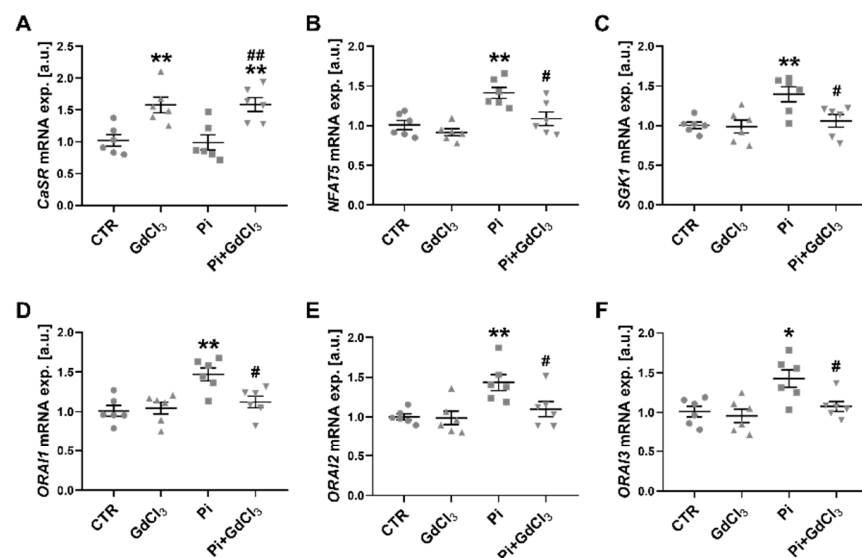


Figure 4. Cont.

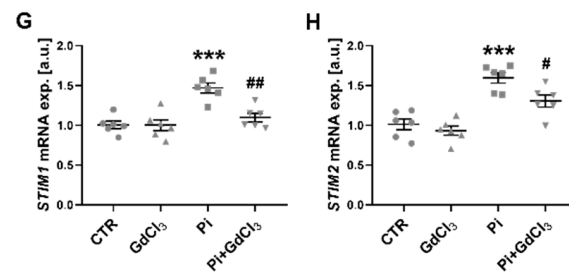


Figure 4. Upregulation of *CaSR* transcription by $GdCl_3$ and reversal of β -glycerophosphate-induced *NEAT5*, *SGK1*, *ORAI1*, *ORAI2*, *ORAI3*, *STIM1* and *STIM2* transcription in megakaryocytes by $GdCl_3$. (A–H) Arithmetic means (\pm SEM, $n = 6$) of *CaSR* (A), *NEAT5* (B), *SGK1* (C), *ORAI1* (D), *ORAI2* (E), *ORAI3* (F), *STIM1* (G) and *STIM2* (H) transcript levels in megakaryocytes without (CTR) and with prior 24-h exposure to 50 μ M $GdCl_3$ alone ($GdCl_3$), 2 mM β -glycerophosphate alone (Pi) or 2 mM β -glycerophosphate and 50 μ M $GdCl_3$ (Pi+ $GdCl_3$). * ($p < 0.05$), ** ($p < 0.01$), *** ($p < 0.001$) indicate statistically significant differences compared to CTR; # ($p < 0.05$), ## ($p < 0.01$) indicate statistically significant differences compared to Pi alone (ANOVA). *CaSR*, calcium-sensing receptor; CTR, control.

As shown in Figure 5, 50 μ M $GdCl_3$ further significantly blunted the β -glycerophosphate-induced upregulation of ORAI1 and STIM1 protein abundance (Figure 5). Again, 50 μ M $GdCl_3$ did not significantly modify the ORAI1 and STIM1 protein abundance in the absence of β -glycerophosphate (Figure 5).

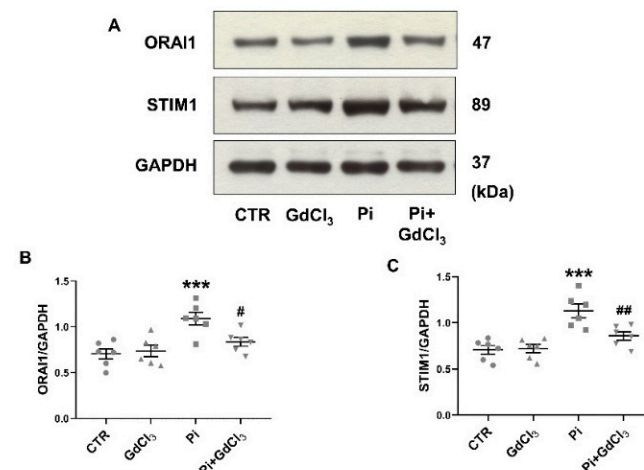


Figure 5. Reversal of β -glycerophosphate-induced ORAI1 and STIM1 protein expression in megakaryocytes by $GdCl_3$. (A) Original Western blots of ORAI1, STIM1 and GAPDH protein abundance in megakaryocytes without (CTR) and with prior 24-h exposure to 50 μ M $GdCl_3$ alone ($GdCl_3$), 2 mM β -glycerophosphate alone (Pi) or 2 mM β -glycerophosphate and 50 μ M $GdCl_3$ (Pi+ $GdCl_3$). (B,C) Arithmetic means \pm SEM ($n = 6$) of ORAI1 (B) and STIM1 (C) protein abundance in megakaryocytes without (CTR) and with prior 24-h exposure to 50 μ M $GdCl_3$ alone ($GdCl_3$), 2 mM β -glycerophosphate alone (Pi) or 2 mM β -glycerophosphate and 50 μ M $GdCl_3$ (Pi+ $GdCl_3$). *** ($p < 0.001$) indicates statistically significant difference compared to CTR; # ($p < 0.05$), ## ($p < 0.01$) indicate statistically significant differences compared to Pi alone (ANOVA). CTR, control.

As illustrated in Figure 6, 50 μ M $GdCl_3$ significantly blunted the β -glycerophosphate-induced upregulation of the SOCE peak and slope without significantly modifying Ca^{2+} release. Again, in the absence of β -glycerophosphate, 50 μ M $GdCl_3$ did not significantly modify SOCE.

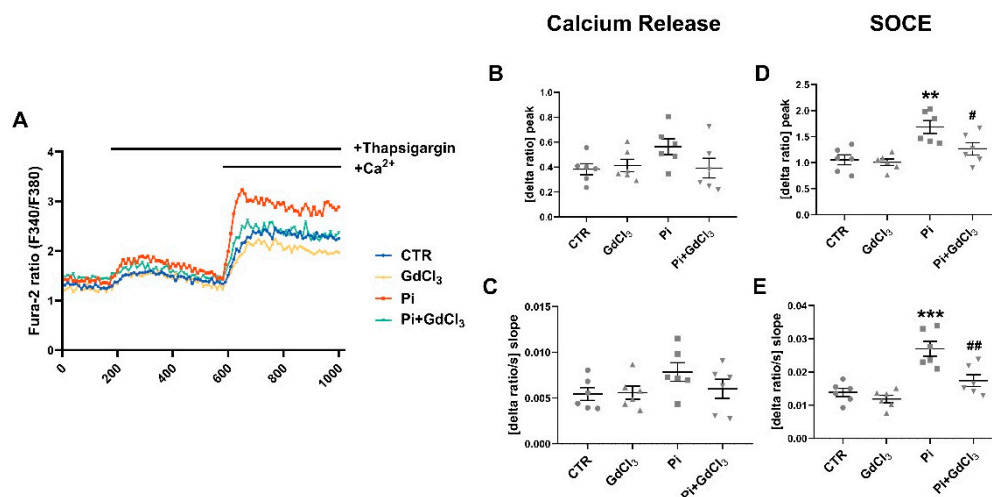


Figure 6. Reversal of β -glycerophosphate-induced increase in store-operated Ca^{2+} entry (SOCE) in megakaryocytes by GdCl_3 . (A) Representative tracings of Fura-2 fluorescence ratio in fluorescence spectrometry before and following extracellular Ca^{2+} removal and addition of thapsigargin ($1 \mu\text{M}$) as well as re-addition of extracellular Ca^{2+} in megakaryocytes without (CTR) or with prior 24-h exposure to $50 \mu\text{M}$ GdCl_3 alone (GdCl_3), 2mM β -glycerophosphate alone (Pi) or 2mM β -glycerophosphate and $50 \mu\text{M}$ GdCl_3 (Pi+ GdCl_3). (B,C) Arithmetic means ($\pm\text{SEM}$, $n = 6$) of peak (B) and slope (C) increase in Fura-2 fluorescence ratio following addition of thapsigargin ($1 \mu\text{M}$) in megakaryocytes without (CTR) or with prior 24-h exposure to $50 \mu\text{M}$ GdCl_3 alone (GdCl_3), 2mM β -glycerophosphate alone (Pi) or 2mM β -glycerophosphate and $50 \mu\text{M}$ GdCl_3 (Pi+ GdCl_3). (D,E) Arithmetic means ($\pm\text{SEM}$, $n = 6$) of peak (D) and slope (E) increase in Fura-2 fluorescence ratio following re-addition of extracellular Ca^{2+} in megakaryocytes without (CTR) or with prior 24-h exposure to $50 \mu\text{M}$ GdCl_3 alone (GdCl_3), 2mM β -glycerophosphate alone (Pi) or 2mM β -glycerophosphate and $50 \mu\text{M}$ GdCl_3 (Pi+ GdCl_3). ** ($p < 0.01$), *** ($p < 0.001$) indicate statistically significant differences compared to CTR; # ($p < 0.05$), ## ($p < 0.01$) indicate statistically significant differences compared to Pi alone (ANOVA). CTR, control.

3. Discussion

The present study confirms previous observations [30] demonstrating the upregulation of NFAT5, ORAI1, ORAI2, ORAI3, STIM1 and STIM2 expression as well as SOCE by the phosphate donor β -glycerophosphate in megakaryocytes.

More importantly, the present study reveals that all those effects were blunted or virtually abolished by 1.5mM MgCl_2 and by $50 \mu\text{M}$ GdCl_3 . MgCl_2 and GdCl_3 are, at least in part, effective by suppression of NFAT5 expression. NFAT5 upregulates the expression of SGK1 [13], which fosters degradation of the inhibitor protein $\text{I}\kappa\text{B}\alpha$ and subsequent nuclear translocation of the transcription factor $\text{NF}\kappa\text{B}$ [15]. $\text{NF}\kappa\text{B}$ is a powerful stimulator of ORAI1 expression [15]. The present observations do not, however, exclude further signaling contributing to the upregulation of ORAI/STIM by β -glycerophosphate and its reversal by MgCl_2 or GdCl_3 in megakaryocytes. It should be pointed out that the signaling shown here is triggered by sustained exposure to MgCl_2 or GdCl_3 . Different signaling elements may prevail following acute stimulation with MgCl_2 or GdCl_3 , such as G protein-dependent activation of phospholipase C and inositol trisphosphate formation, as shown in other cell types [38–43].

Without β -glycerophosphate treatment, the addition of $50 \mu\text{M}$ GdCl_3 did not significantly modify SOCE (Figure 6). The possibility should be considered that CaSR activation disrupts the upregulation of ORAI by β -glycerophosphate/ $\text{NFAT5}/\text{NF}\kappa\text{B}$ but does not modify basal ORAI expression. However, the scatter of the data does not allow exclusion of minor effects.

ORAI and STIM participate in the orchestration of platelet activation [44]. At least in theory, inhibition of ORAI and STIM expression and SOCE could contribute to the previously observed inhibition of platelet activity by CaSR activation in hyperhomocysteinemia [37]. Moreover, in view of the present observations and the known role of platelets

in the pathophysiology of cardiac infarction and stroke [45], CaSR activation could counteract upregulation of platelet activity by phosphate and thus reduce the risk of cardiac infarction and stroke in CKD patients [46,47]. Clearly, additional experimental effort and clinical studies are required to define the potentially protective effect of CaSR agonists on pathological platelet activity in CKD.

In conclusion, the activation of CaSR by $MgCl_2$ and $GdCl_3$ reverses the upregulation of NFAT5, SGK1, ORAI1, ORAI2, ORAI3, STIM1 and STIM2 expression as well as SOCE by the phosphate donor β -glycerophosphate in megakaryocytes (Figure 7). The effect may decrease the cardiovascular risk in hyperphosphatemic chronic kidney disease patients.

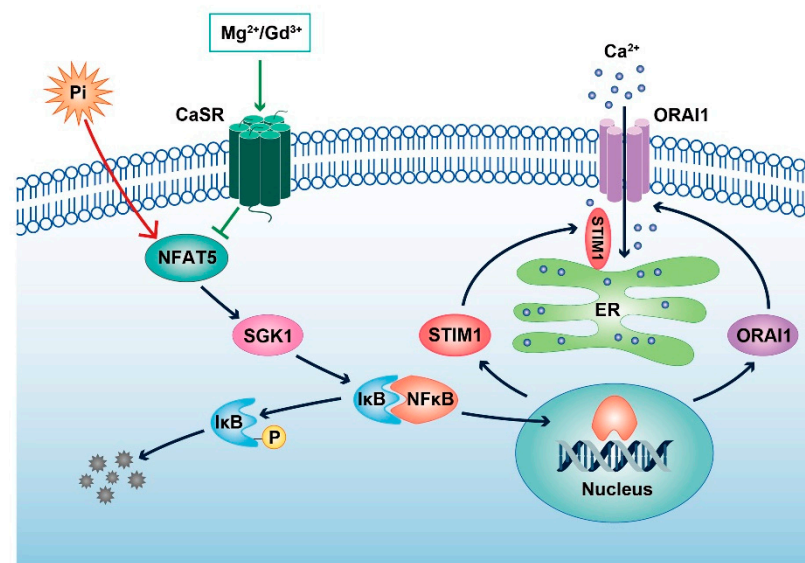


Figure 7. Mg^{2+} and Gd^{3+} interfere with phosphate-induced SOCE upregulation by the activation of CaSR in megakaryocytes—a schematic representation. In megakaryocytes, the phosphate donor β -glycerophosphate upregulates NFAT5 and SGK1 expression, which leads to the degradation of the NF κ B inhibitory protein I κ B with subsequent nuclear translocation of NF κ B and NF κ B-dependent transcription of ORAI1 and STIM1. CaSR can be activated by cations such as Mg^{2+} and Gd^{3+} and inhibits phosphate-induced SOCE enhancement, at least partially, via the downregulation of the signaling pathway. CaSR, calcium-sensing receptor; ER, endoplasmic reticulum.

4. Materials and Methods

4.1. Cell Culture

Human megakaryocytic cells (Meg-01) from American Type Culture Collection (ATCC, Manassas, VA, USA) were cultured in RPMI 1640 (Roswell Park Memorial Institute medium, Gibco, Paisley, UK) containing 10% fetal bovine serum (FBS, Gibco, Paisley, United Kingdom) and 1% Penicillin/Streptomycin in a humidified incubator at 37°C and 5% CO_2 . Where indicated, the cells were exposed to 2 mM β -glycerophosphate (Sigma, Steinheim, Germany) for 24 h in the absence and presence of 1.5 mM $MgCl_2$ or 50 μ M $GdCl_3$ (Sigma, Steinheim, Germany). In analysis of vascular calcification, phosphate donor β -glycerophosphate is widely used as a substitute for phosphate and a well-established stimulator of tissue calcification [48–50].

4.2. Quantitative PCR

To determine transcript levels of *CaSR*, *NFAT5*, *SGK1*, *ORAI1*, *ORAI2*, *ORAI3*, *STIM1* and *STIM2*, total RNA was extracted according to the manufacturer's instructions with TriFast (Peqlab, Erlangen, Germany) [16,51–54]. DNase digestion was performed to avoid DNA contamination and was followed by reverse transcription using Oligo(dT)15 primers (Promega, Mannheim, Germany) and the GoScript reverse transcription system (Promega,

Mannheim, Germany). Real-time polymerase chain reaction (RT-PCR) amplification of the respective genes was set up in a total volume of 15 μ L using 100 ng of cDNA, 500 nM forward and reverse primers and 2 \times GoTaq[®] qPCR Master Mix (Promega, Hilden, Germany) following the manufacturer's protocol. Cycling conditions were as follows: initial denaturation at 95 °C for 3 min, followed by 40 cycles of 95 °C for 15 s, 60 °C for 30 s and 72 °C for 30 s. The primers used for amplification in this study are given in Table 1 (Invitrogen, Darmstadt, Germany).

Table 1. List of the primer sequences for RT-PCR.

Name	Orientation	Sequence
<i>GAPDH</i>	Forward	5'-TCAAGGCTGAGAACGGGAAG-3'
	Reverse	5'-TGGACTCCACGACGTACTCA-3'
<i>CaSR</i>	Forward	5'-ATGCCAAGAAGGGAGAAAGACTCTT-3'
	Reverse	5'-TCAGGACACTCCACACTCAAAG-3'
<i>NEAT5</i>	Forward	5'-GGGTCAAACGACGAGATTGTG-3'
	Reverse	5'-GTCCGTGGTAAGCTGAGAAAG-3'
<i>SGK1</i>	Forward	5'-AGGAGGATGGGTCTGAACGA-3'
	Reverse	5'-GGGCCAAGGTTGATTGCTG-3'
<i>ORAI1</i>	Forward	5'-CACCTGTTTGCCTCATGAT-3'
	Reverse	5'-GGGACTCCTTGACCGAGTTG-3'
<i>ORAI2</i>	Forward	5'-CAGCTCCGGGAAGGAACGTC-3'
	Reverse	5'-CTCCATCCCATCTCCTTGCG-3'
<i>ORAI3</i>	Forward	5'-CTTCCAATCTCCCACGGTCC-3'
	Reverse	5'-GTTCTGCTTGTAGCGGTCT-3'
<i>STIM1</i>	Forward	5'-AAGAAGGCATTACTGGCGCT-3'
	Reverse	5'-GATGGTGTGCTGGGTCTGG-3'
<i>STIM2</i>	Forward	5'-AGGGGATTCGCCTGTAAGTCTG-3'
	Reverse	5'-GGTTTACTGTCGTTGCCAGC-3'

Melting curves were analyzed to confirm PCR product specificity. The CFX96 Real-Time System (BioRad, Munich, Germany) was used to perform real-time PCR amplifications. All experiments were conducted in duplicate. Relative mRNA expression was calculated by the $2^{-\Delta\Delta CT}$ method using the housekeeping gene Glyceraldehyde 3-phosphate dehydrogenase (*GAPDH*) as internal reference, normalized to the control group.

4.3. Western Blotting

Protein abundance of ORAI1, STIM1 and GAPDH was determined by Western blotting [16,51–54]. Megakaryocyte suspensions were centrifuged for 5 min at 300 \times g and 4 °C. The pellet was washed with ice-cold PBS and suspended in 40 μ L ice-cold RIPA lysis buffer (Cell Signaling Technology, Danvers, MA, USA) containing Protease Inhibitor Cocktail (Thermo-Fisher Scientific, Waltham, MA, USA). After centrifugation (20,000 \times g, 4 °C for 20 min), the supernatant was taken to determine protein concentration using the Bradford assay (BioRad, Munich, Germany). For Western blotting, 30 μ g of proteins was electro-transferred onto a poly-vinylidene difluoride (PVDF) membrane after electrophoresis using 10% SDS-PAGE and blocked with 5% milk in TBST at room temperature for 1 h. The membranes were incubated with primary anti-ORAI1 antibody (1:1000, Proteintech, Chicago, IL, USA), anti-STIM1 antibody (1:1000, Cell Signaling Technology, Danvers, MA, USA) and anti-GAPDH antibody (1:2000, Cell Signaling Technology, Danvers, MA, USA) at 4 °C overnight. After washing (TBST), the blots were incubated with secondary anti-rabbit antibody conjugated with horseradish peroxidase (1:2000, Cell Signaling Technology, Danvers, MA, USA) for 2 h at room temperature. Protein bands were detected after additional washes (TBST) with an ECL detection reagent (Thermo-Fisher Scientific, Waltham, MA, USA). For densitometry image analysis, Western blots were scanned and analyzed by

ImageJ software (Version 1.52, NIH, Bethesda, MD, USA). The results are shown as the ratio of total protein to GAPDH. Protein-Marker (Thermo-Fisher Scientific, Waltham, MA, USA) was used as reference to assign the right protein size.

4.4. Cytosolic Calcium Measurements

To determine the cytosolic Ca^{2+} concentration ($[\text{Ca}^{2+}]_i$), Fura-2 fluorescence was utilized [16,51–55]. Cells were preincubated for 30–45 min with Fura-2/AM (2 μM , Invitrogen, Goettingen, Germany) at 37 °C and excited alternatively at 340 nm and 380 nm in an inverted phase-contrast microscope (Axiovert 100, Zeiss, Oberkochen, Germany) through an objective (Fluor 40 \times /1.30 oil). At 505 nm, the emitted fluorescence intensity was recorded. Data (6/minute) were acquired using computer software Metafluor (Version 7.5, Universal Imaging, Downingtown, PA, USA). To estimate cytosolic Ca^{2+} activity, ratiometer (340 nm/380 nm)-based analysis was employed. SOCE was determined following extracellular Ca^{2+} removal causing store depletion and subsequent Ca^{2+} re-addition in constant presence of SERCA inhibitor thapsigargin (1 μM , Invitrogen, Goettingen, Germany). For quantification of Ca^{2+} entry, the slope (delta ratio/s) and peak (delta ratio) were determined following re-addition of Ca^{2+} . Experiments were performed with HEPES solution containing (in mM): 125 NaCl, 5 KCl, 1.2 MgSO_4 , 2 Na_2HPO_4 , 32 HEPES, 5 glucose, 1 CaCl_2 , pH 7.4. Ca^{2+} -free conditions were achieved by using Ca^{2+} -free HEPES solution containing (in mM): 125 NaCl, 5 KCl, 1.2 MgSO_4 , 2 Na_2HPO_4 , 32 HEPES, 5 glucose, 0.5 EGTA, pH 7.4.

4.5. Statistical Analysis

Statistical analysis was conducted using SPSS software (Version 25.0, SPSS Inc., Chicago, IL, USA). Data are provided as means \pm SEM, and n represents the number of independent experiments (i.e., in fluorescence experiments, the number of dishes measured). All data were tested for significance using Student's t test or ANOVA. Results with $p < 0.05$ were considered statistically significant.

Supplementary Materials: Supplementary materials can be found at <https://www.mdpi.com/1422-0067/22/7/3292/s1>.

Author Contributions: F.L., B.N. and M.G. designed the research; K.Z. and X.Z. performed experiments; K.Z., X.Z., K.M., J.L. and F.L. analyzed and interpreted the data; F.L. drafted the manuscript. All authors have read and agreed to the published version of the manuscript.

Funding: The study was supported in part by the Open Access Publishing Fund of Tübingen University, by grants from the Deutsche Forschungsgemeinschaft (DFG) NU 53/12-2 and NU 53/13-1 to B.N. and by DFG project number 374031971–TRR 240 to M.G.; K.Z., X.Z. and J.L. were supported by the Chinese Scholarship Council. The sponsor(s) had no role in the study design, the collection, analysis and interpretation of data, in the writing of the report or in the decision to submit the article for publication.

Data Availability Statement: The data presented in this study are available on request from the corresponding author.

Acknowledgments: The authors gratefully acknowledge the meticulous preparation of the manuscript by Lejla Subasic.

Conflicts of Interest: The authors declare no conflict of interest.

References

1. Kapustin, A.N.; Chatrou, M.L.; Drozdov, I.; Zheng, Y.; Davidson, S.M.; Soong, D.; Furmanik, M.; Sanchis, P.; De Rosales, R.T.; Alvarez-Hernandez, D.; et al. Vascular smooth muscle cell calcification is mediated by regulated exosome secretion. *Circ. Res.* **2015**, *116*, 1312–1323. [CrossRef]
2. Lang, F.; Ritz, E.; Alesutan, I.; Voelkl, J. Impact of aldosterone on osteoinductive signaling and vascular calcification. *Nephron. Physiol.* **2014**, *128*, 40–45. [CrossRef]
3. Lang, F.; Ritz, E.; Voelkl, J.; Alesutan, I. Vascular calcification—is aldosterone a culprit? *Nephrol. Dial. Transpl.* **2013**, *28*, 1080–1084. [CrossRef]

4. Steitz, S.A.; Speer, M.Y.; Curinga, G.; Yang, H.Y.; Haynes, P.; Aebersold, R.; Schinke, T.; Karsenty, G.; Giachelli, C.M. Smooth muscle cell phenotypic transition associated with calcification: Upregulation of *Cbfa1* and downregulation of smooth muscle lineage markers. *Circ Res.* **2001**, *89*, 1147–1154. [[CrossRef](#)] [[PubMed](#)]
5. Blacher, J.; Guerin, A.P.; Pannier, B.; Marchais, S.J.; London, G.M. Arterial calcifications, arterial stiffness, and cardiovascular risk in end-stage renal disease. *Hypertension* **2001**, *38*, 938–942. [[CrossRef](#)]
6. London, G.M.; Guerin, A.P.; Marchais, S.J.; Metivier, F.; Pannier, B.; Adda, H. Arterial media calcification in end-stage renal disease: Impact on all-cause and cardiovascular mortality. *Nephrol. Dial. Transpl.* **2003**, *18*, 1731–1740. [[CrossRef](#)] [[PubMed](#)]
7. Mizobuchi, M.; Towler, D.; Slatopolsky, E. Vascular calcification: The killer of patients with chronic kidney disease. *J. Am. Soc. Nephrol.* **2009**, *20*, 1453–1464. [[CrossRef](#)] [[PubMed](#)]
8. Foley, R.N.; Parfrey, P.S.; Sarnak, M.J. Epidemiology of cardiovascular disease in chronic renal disease. *J. Am. Soc. Nephrol.* **1998**, *9*, S16–S23. [[CrossRef](#)]
9. Alesutan, I.; Musculus, K.; Castor, T.; Alzoubi, K.; Voelkl, J.; Lang, F. Inhibition of Phosphate-Induced Vascular Smooth Muscle Cell Osteo-/Chondrogenic Signaling and Calcification by Bafilomycin A1 and Methylamine. *Kidney Blood Press Res.* **2015**, *40*, 490–499. [[CrossRef](#)]
10. Feger, M.; Alesutan, I.; Castor, T.; Mia, S.; Musculus, K.; Voelkl, J.; Lang, F. Inhibitory effect of NH₄Cl treatment on renal Tgfss1 signaling following unilateral ureteral obstruction. *Cell Physiol. Biochem.* **2015**, *37*, 955–964. [[CrossRef](#)] [[PubMed](#)]
11. Lang, F.; Guelinckx, I.; Lemetais, G.; Melander, O. Two Liters a Day Keep the Doctor Away? Considerations on the Pathophysiology of Suboptimal Fluid Intake in the Common Population. *Kidney Blood Press Res.* **2017**, *42*, 483–494. [[CrossRef](#)]
12. Leibrock, C.B.; Alesutan, I.; Voelkl, J.; Pakladok, T.; Michael, D.; Schleicher, E.; Kamyabi-Moghaddam, Z.; Quintanilla-Martinez, L.; Kuro-o, M.; Lang, F. NH₄Cl Treatment Prevents Tissue Calcification in *Klotho* Deficiency. *J. Am. Soc. Nephrol.* **2015**, *26*, 2423–2433. [[CrossRef](#)]
13. Chen, S.; Grigsby, C.L.; Law, C.S.; Ni, X.; Nekrep, N.; Olsen, K.; Humphreys, M.H.; Gardner, D.G. Tonicity-dependent induction of *Sgk1* expression has a potential role in dehydration-induced natriuresis in rodents. *J. Clin. Investig.* **2009**, *119*, 1647–1658. [[CrossRef](#)] [[PubMed](#)]
14. Lang, F.; Stourmaras, C.; Zacharopoulou, N.; Voelkl, J.; Alesutan, I. Serum- and glucocorticoid-inducible kinase 1 and the response to cell stress. *Cell Stress* **2018**, *3*, 1–8. [[CrossRef](#)]
15. Lang, F.; Shumilina, E. Regulation of ion channels by the serum- and glucocorticoid-inducible kinase SGK1. *FASEB J.* **2013**, *27*, 3–12. [[CrossRef](#)] [[PubMed](#)]
16. Ma, K.; Liu, P.; Al-Maghout, T.; Sukkar, B.; Cao, H.; Voelkl, J.; Alesutan, I.; Pieske, B.; Lang, F. Phosphate-induced ORAI1 expression and store-operated Ca(2+) entry in aortic smooth muscle cells. *J. Mol. Med.* **2019**, *97*, 1465–1475. [[CrossRef](#)]
17. Zhu, X.; Ma, K.; Zhou, K.; Voelkl, J.; Alesutan, I.; Leibrock, C.; Nurnberg, B.; Lang, F. Reversal of phosphate-induced ORAI1 expression, store-operated Ca(2+) entry and osteogenic signaling by MgCl₂ in human aortic smooth muscle cells. *Biochem. Biophys. Res. Commun.* **2020**, *523*, 18–24. [[CrossRef](#)]
18. Ma, K.; Sukkar, B.; Zhu, X.; Zhou, K.; Cao, H.; Voelkl, J.; Alesutan, I.; Nurnberg, B.; Lang, F. Stimulation of ORAI1 expression, store-operated Ca(2+) entry, and osteogenic signaling by high glucose exposure of human aortic smooth muscle cells. *Pflug. Arch. Eur. J. Physiol.* **2020**, *472*, 1093–1102. [[CrossRef](#)] [[PubMed](#)]
19. Lee, S.H.; Park, Y.; Song, M.; Srikanth, S.; Kim, S.; Kang, M.K.; Gwack, Y.; Park, N.H.; Kim, R.H.; Shin, K.H. *Orai1* mediates osteogenic differentiation via BMP signaling pathway in bone marrow mesenchymal stem cells. *Biochem. Biophys. Res. Commun.* **2016**, *473*, 1309–1314. [[CrossRef](#)]
20. Eckstein, M.; Vaeth, M.; Aulestia, F.J.; Costiniti, V.; Kassam, S.N.; Bromage, T.G.; Pedersen, P.; Issekutz, T.; Idaghdour, Y.; Moursi, A.M.; et al. Differential regulation of Ca(2+) influx by ORAI channels mediates enamel mineralization. *Sci. Signal.* **2019**, *12*. [[CrossRef](#)]
21. McCarl, C.A.; Picard, C.; Khalil, S.; Kawasaki, T.; Rother, J.; Papolos, A.; Kutok, J.; Hivroz, C.; Ledest, F.; Plogmann, K.; et al. ORAI1 deficiency and lack of store-operated Ca²⁺ entry cause immunodeficiency, myopathy, and ectodermal dysplasia. *J. Allergy Clin. Immunol.* **2009**, *124*, 1311–1318.e1317. [[CrossRef](#)]
22. Braun, A.; Varga-Szabo, D.; Kleinschnitz, C.; Pleines, I.; Bender, M.; Austinat, M.; Bosl, M.; Stoll, G.; Nieswandt, B. *Orai1* (CRACM1) is the platelet SOC channel and essential for pathological thrombus formation. *Blood* **2009**, *113*, 2056–2063. [[CrossRef](#)] [[PubMed](#)]
23. Lang, F.; Munzer, P.; Gawaz, M.; Borst, O. Regulation of STIM1/*Orai1*-dependent Ca²⁺ signalling in platelets. *Thromb. Haemost.* **2013**, *110*, 925–930. [[CrossRef](#)]
24. Eyllenstein, A.; Gehring, E.M.; Heise, N.; Shumilina, E.; Schmidt, S.; Szteyn, K.; Munzer, P.; Nurbaeva, M.K.; Eichenmuller, M.; Tyán, L.; et al. Stimulation of Ca²⁺-channel *Orai1*/STIM1 by serum- and glucocorticoid-inducible kinase 1 (SGK1). *FASEB J.* **2011**, *25*, 2012–2021. [[CrossRef](#)] [[PubMed](#)]
25. Borst, O.; Schmidt, E.M.; Munzer, P.; Schonberger, T.; Towhid, S.T.; Elvers, M.; Leibrock, C.; Schmid, E.; Eyllenstein, A.; Kuhl, D.; et al. The serum- and glucocorticoid-inducible kinase 1 (SGK1) influences platelet calcium signaling and function by regulation of *Orai1* expression in megakaryocytes. *Blood* **2012**, *119*, 251–261. [[CrossRef](#)]
26. Lang, F.; Gawaz, M.; Borst, O. The serum- & glucocorticoid-inducible kinase in the regulation of platelet function. *Acta Physiol.* **2015**, *213*, 181–190. [[CrossRef](#)]

27. Sahu, I.; Pelzl, L.; Sukkar, B.; Fakhri, H.; Al-Maghout, T.; Cao, H.; Hauser, S.; Gutti, R.; Gawaz, M.; Lang, F. NFAT5-sensitive Orai1 expression and store-operated Ca(2+) entry in megakaryocytes. *FASEB J.* **2017**, *31*, 3439–3448. [[CrossRef](#)]
28. Balduini, A.; Badalucco, S.; Pugliano, M.T.; Baev, D.; De Silvestri, A.; Cattaneo, M.; Rosti, V.; Barosi, G. In vitro megakaryocyte differentiation and proplatelet formation in Ph-negative classical myeloproliferative neoplasms: Distinct patterns in the different clinical phenotypes. *PLoS ONE* **2011**, *6*, e21015. [[CrossRef](#)]
29. Golfier, S.; Kondo, S.; Schulze, T.; Takeuchi, T.; Vassileva, G.; Achtman, A.H.; Graler, M.H.; Abbondanzo, S.J.; Wiekowski, M.; Kremmer, E.; et al. Shaping of terminal megakaryocyte differentiation and proplatelet development by sphingosine-1-phosphate receptor S1P4. *FASEB J.* **2010**, *24*, 4701–4710. [[CrossRef](#)]
30. Pelzl, L.; Sahu, I.; Ma, K.; Heinzmann, D.; Bhuyan, A.A.M.; Al-Maghout, T.; Sukkar, B.; Sharma, Y.; Marini, I.; Rigoni, F.; et al. Beta-Glycerophosphate-Induced ORAI1 Expression and Store Operated Ca(2+) Entry in Megakaryocytes. *Sci. Rep.* **2020**, *10*, 1728. [[CrossRef](#)]
31. Di Buduo, C.A.; Moccia, F.; Battiston, M.; De Marco, L.; Mazzucato, M.; Moratti, R.; Tanzi, F.; Balduini, A. The importance of calcium in the regulation of megakaryocyte function. *Haematologica* **2014**, *99*, 769–778. [[CrossRef](#)] [[PubMed](#)]
32. Somasundaram, B.; Mahaut-Smith, M.P. Three cation influx currents activated by purinergic receptor stimulation in rat megakaryocytes. *J. Physiol.* **1994**, *480*, 225–231. [[CrossRef](#)]
33. Somasundaram, B.; Mason, M.J.; Mahaut-Smith, M.P. Thrombin-dependent calcium signalling in single human erythroleukaemia cells. *J. Physiol.* **1997**, *501*, 485–495. [[CrossRef](#)] [[PubMed](#)]
34. Tolhurst, G.; Carter, R.N.; Amisten, S.; Holdich, J.P.; Erlinge, D.; Mahaut-Smith, M.P. Expression profiling and electrophysiological studies suggest a major role for Orai1 in the store-operated Ca²⁺ influx pathway of platelets and megakaryocytes. *Platelets* **2008**, *19*, 308–313. [[CrossRef](#)]
35. Alesutan, I.; Tuffaha, R.; Auer, T.; Feger, M.; Pieske, B.; Lang, F.; Voelkl, J. Inhibition of osteo/chondrogenic transformation of vascular smooth muscle cells by MgCl₂ via calcium-sensing receptor. *J. Hypertens.* **2017**, *35*, 523–532. [[CrossRef](#)] [[PubMed](#)]
36. House, M.G.; Kohlmeier, L.; Chattopadhyay, N.; Kifor, O.; Yamaguchi, T.; Leboff, M.S.; Glowacki, J.; Brown, E.M. Expression of an extracellular calcium-sensing receptor in human and mouse bone marrow cells. *J. Bone Miner. Res. Off. J. Am. Soc. Bone Miner. Res.* **1997**, *12*, 1959–1970. [[CrossRef](#)] [[PubMed](#)]
37. Wang, Y.; Zhao, Z.; Shi, S.; Gao, F.; Wu, J.; Dong, S.; Zhang, W.; Liu, Y.; Zhong, X. Calcium sensing receptor initiating cystathionine-gamma-lyase/hydrogen sulfide pathway to inhibit platelet activation in hyperhomocysteinemia rat. *Exp. Cell Res.* **2017**, *358*, 171–181. [[CrossRef](#)]
38. Zhang, W.; Sun, R.; Zhong, H.; Tang, N.; Liu, Y.; Zhao, Y.; Zhang, T.; He, F. CaSR participates in the regulation of vascular tension in the mesentery of hypertensive rats via the PLCIP3/ACV/cAMP/RAS pathway. *Mol. Med. Rep.* **2019**, *20*, 4433–4448. [[CrossRef](#)]
39. Guo, S.; Yan, T.; Shi, L.; Liu, A.; Zhang, T.; Xu, Y.; Jiang, W.; Yang, Q.; Yang, L.; Liu, L.; et al. Matrine, as a CaSR agonist promotes intestinal GLP-1 secretion and improves insulin resistance in diabetes mellitus. *Phytomedicine* **2021**, *84*, 153507. [[CrossRef](#)]
40. Maltsev, A.V. Agmatine modulates calcium handling in cardiomyocytes of hibernating ground squirrels through calcium-sensing receptor signaling. *Cell Signal.* **2018**, *51*, 1–12. [[CrossRef](#)]
41. Ortiz-Capisano, M.C.; Reddy, M.; Mendez, M.; Garvin, J.L.; Beierwaltes, W.H. Juxtaglomerular cell CaSR stimulation decreases renin release via activation of the PLC/IP(3) pathway and the ryanodine receptor. *Am. J. Physiol. Ren. Physiol.* **2013**, *304*, F248–F256. [[CrossRef](#)]
42. Kwak, J.O.; Kwak, J.; Kim, H.W.; Oh, K.J.; Kim, Y.T.; Jung, S.M.; Cha, S.H. The extracellular calcium sensing receptor is expressed in mouse mesangial cells and modulates cell proliferation. *Exp. Mol. Med.* **2005**, *37*, 457–465. [[CrossRef](#)]
43. Hattori, T.; Ara, T.; Fujinami, Y. Pharmacological evidences for the stimulation of calcium-sensing receptors by nifedipine in gingival fibroblasts. *J. Pharm. Pharm.* **2011**, *2*, 30–35. [[CrossRef](#)]
44. Berna-Erro, A.; Jardin, I.; Smani, T.; Rosado, J.A. Regulation of Platelet Function by Orai, STIM and TRP. *Adv. Exp. Med. Biol.* **2016**, *898*, 157–181. [[CrossRef](#)]
45. Renga, B.; Scavizzi, F. Platelets and cardiovascular risk. *Acta Cardiol* **2017**, *72*, 2–8. [[CrossRef](#)]
46. Moody, W.E.; Edwards, N.C.; Chue, C.D.; Ferro, C.J.; Townend, J.N. Arterial disease in chronic kidney disease. *Heart* **2013**, *99*, 365–372. [[CrossRef](#)]
47. Webster, A.C.; Nagler, E.V.; Morton, R.L.; Masson, P. Chronic Kidney Disease. *Lancet* **2017**, *389*, 1238–1252. [[CrossRef](#)]
48. Giachelli, C.M.; Jono, S.; Shioi, A.; Nishizawa, Y.; Mori, K.; Morii, H. Vascular calcification and inorganic phosphate. *Am. J. Kidney Dis.* **2001**, *38*, S34–S37. [[CrossRef](#)]
49. Shioi, A.; Nishizawa, Y.; Jono, S.; Koyama, H.; Hosoi, M.; Morii, H. Beta-glycerophosphate accelerates calcification in cultured bovine vascular smooth muscle cells. *Arter. Thromb. Vasc. Biol.* **1995**, *15*, 2003–2009. [[CrossRef](#)]
50. Moe, S.M.; Chen, N.X. Pathophysiology of vascular calcification in chronic kidney disease. *Circ. Res.* **2004**, *95*, 560–567. [[CrossRef](#)]
51. Abdelazeem, K.N.M.; Droppova, B.; Sukkar, B.; Al-Maghout, T.; Pelzl, L.; Zacharopoulou, N.; Ali Hassan, N.H.; Abdel-Fattah, K.I.; Stournaras, C.; Lang, F. Upregulation of Orai1 and STIM1 expression as well as store-operated Ca(2+) entry in ovary carcinoma cells by placental growth factor. *Biochem. Biophys. Res. Commun.* **2019**, *512*, 467–472. [[CrossRef](#)]
52. Zhang, S.; al-Maghout, T.; Bissinger, R.; Zeng, N.; Pelzl, L.; Salker, M.S.; Cheng, A.; Singh, Y.; Lang, F. Epigallocatechin-3-gallate (EGCG) up-regulates miR-15b expression thus attenuating store operated calcium entry (SOCE) into murine CD4+ T cells and human leukaemic T cell lymphoblasts. *Oncotarget* **2017**, *8*, 89500. [[CrossRef](#)] [[PubMed](#)]

53. Pelzl, L.; Hauser, S.; Elsir, B.; Sukkar, B.; Sahu, I.; Singh, Y.; Hoflinger, P.; Bissinger, R.; Jemaa, M.; Stournaras, C.; et al. Lithium Sensitive ORAI1 Expression, Store Operated Ca(2+) Entry and Suicidal Death of Neurons in Chorea-Acanthocytosis. *Sci. Rep.* **2017**, *7*, 6457. [[CrossRef](#)]
54. Sukkar, B.; Hauser, S.; Pelzl, L.; Hosseinzadeh, Z.; Sahu, I.; Al-Maghout, T.; Bhuyan, A.A.M.; Zacharopoulou, N.; Stournaras, C.; Schols, L.; et al. Inhibition of Lithium Sensitive Orail/STIM1 Expression and Store Operated Ca²⁺ Entry in Chorea-Acanthocytosis Neurons by NF-kappaB Inhibitor Wogonin. *Cell Physiol. Biochem.* **2018**, *51*, 278–289. [[CrossRef](#)]
55. Schmid, E.; Bhandaru, M.; Nurbaeva, M.K.; Yang, W.; Sztelyn, K.; Russo, A.; Leibrock, C.; Tyan, L.; Pearce, D.; Shumilina, E.; et al. SGK3 regulates Ca(2+) entry and migration of dendritic cells. *Cell Physiol. Biochem.* **2012**, *30*, 1423–1435. [[CrossRef](#)]